Polarization Entanglement by Time-Reversed Hong-Ou-Mandel Interference

Yuanyuan Chen,[1,2,3,*] Sebastian Ecker,[1,2] Sören Wengerowsky,[1,2] Lukas Bulla,[1,2]
Siddarth Koduru Joshi,[1,2,†] Fabian Steinlechner,[1,2] and Rupert Ursin[1,2,‡]

[1]*Institute for Quantum Optics and Quantum Information–Vienna (IQOQI), Austrian Academy of Sciences, Boltzmanngasse 3, 1090 Vienna, Austria*

[2]*Vienna Center for Quantum Science and Technology (VCQ), Faculty of Physics, University of Vienna, Boltzmanngasse 5, 1090 Vienna, Austria*

[3]*State Key Laboratory for Novel Software Technology, Nanjing University, Xianlin Avenue 163, Nanjing 210046, China*

(Received 29 June 2018; published 14 November 2018)

Sources of entanglement are an enabling resource in quantum technology, and pushing the limits of generation rate and quality of entanglement is a necessary prerequisite towards practical applications. Here, we present an ultrabright source of polarization-entangled photon pairs based on time-reversed Hong-Ou-Mandel interference. By superimposing four pair-creation possibilities on a polarization beam splitter, pairs of identical photons are separated into two spatial modes without the usual requirement for wavelength distinguishability or noncollinear emission angles. Our source yields high-fidelity polarization entanglement and high pair-generation rates without any requirement for active interferometric stabilization, which makes it an ideal candidate for a variety of applications, in particular those requiring indistinguishable photons.

DOI: 10.1103/PhysRevLett.121.200502

Introduction.—Quantum entanglement is an enabling resource for quantum information processing, and an efficient source of entangled photons can now be considered an absolute necessity in the quantum mechanic's toolkit. Entangled photons can be generated using a variety of technological approaches [1], with spontaneous parametric down-conversion (SPDC) in nonlinear materials representing the present-day gold standard with respect to fiber coupling efficiency [2,3], entangled photon pair rates [4], and entanglement fidelity [5]. In the SPDC process, photons from a strong pump laser (p) spontaneously decay into two daughter photons, commonly referred to as signal (s) and idler (i), which can be tailored to exhibit entanglement in various photonic degrees of freedom. SPDC offers a wide range of possibilities to generate polarization entanglement [6–12], with two widely used source configurations being the crossed-crystal scheme, in which two parametric down-converters, rotated by 90° with respect to each other, are placed in sequence and pumped with a diagonally polarized pump laser [7], and the Sagnac scheme, where a single down-converter is bidirectionally pumped inside a polarization Sagnac interferometer [8,10]. These schemes owe their popularity to the fact that no active interferometric stabilization is required, due to the common path configuration for down-converted and pump photons.

The past two decades have seen significant efforts dedicated to improving the efficiency and tunability of SPDC sources. In particular, the advent of periodic poling technology has greatly extended the range of possible SPDC configurations, and made it possible to engineer highly efficient collinear quasiphase matching (QPM) in long periodically poled nonlinear crystals [4,10,11,13–17] and waveguide structures [18–23]. In particular, SPDC sources that exploit the strong nonlinear interaction of collinear QPM with copolarized pump, signal, and idler photons, so-called type-0 QPM, have resulted in the highest entangled pair rates reported to date [4,24]. Because of the spatial overlap of the SPDC and pump modes, however, these type-0 sources typically require wavelength distinguishability ($\lambda_s \neq \lambda_i$) or noncollinear SPDC emission angles in order to route photons into distinct spatial modes for independent manipulation (e.g., using dichroic mirrors or fiber-Bragg gratings). As this limits their applicability in quantum information processing protocols that require indistinguishable photons, the question naturally arises of how we may generate polarization-entanglement such that identical signal and idler photons are separated deterministically. That is, conditional on the detection of a signal (idler) photon in one spatial mode, there should be, in principle, a unit probability of a corresponding detection of the idler (signal) photon in a conjugate spatial mode. In contrast to this ideal case, the widely used probabilistic separation on a beam splitter always results in an undesirable two-photon component in its output ports.

To tackle this issue, Chen *et al.* [25] proposed a deterministic *quantum splitter* that uses two-photon interference to passively route photons into two spatial modes.

The most widely known manifestation of two-photon interference is the Hong-Ou-Mandel (HOM) effect, where identical photons impinging on the input ports of a beam splitter bunch into either one or the other output port. In a time-reversed analogy, interference of two indistinguishable photon pairs results in antibunching in the output ports of the beam splitter, i.e., a suppression of two-photon components in each port. This quantum splitter approach has since found applications in several experiments, in particular on integrated waveguide platforms [26,27].

Here we present a novel source configuration which exploits time-reversed HOM interference to deterministically route wavelength-degenerate polarization-entangled photons into two distinct spatial modes. By coherent superposition of identical photon pairs in four different modes on a polarization beam splitter (PBS), our source yields polarization entanglement without any requirement for detection postselection. This is achieved in a phase-stable manner by combining the benefits of the popular polarization Sagnac sources and crossed-crystal sources. Using highly efficient collinear type-0 QPM in bulk periodically poled potassium titanyl phosphate (ppKTP) crystals, we generate wavelength-degenerate photon pairs around 810 nm with a Bell-state fidelity of 99.2% and detect a pair rate of 160 kcps per mW of pump power.

This photon pair yield, which—to the best of our knowledge—is the highest value reported for a wavelength-degenerate polarization-entangled photon source, is of particular relevance whenever the available pump power is limited, as is the case in space-proof entangled photon sources for satellite-based quantum communication [28–30], or fundamental tests of quantum theory in scenarios with extreme link loss [31–33]. Moreover, the scheme can be extended to integrated source platforms, where the separation of photons generated in overlapping, copropagating spatial modes is particularly challenging.

Basic scheme.—To illustrate the operational principle of the source (Fig. 1), let us consider a pair of identical photons which are both linearly polarized either along the diagonal or antidiagonal direction. The photons are incident on a polarization beam splitter in a state

$$\frac{(a_D^{\dagger 2} + e^{i\phi} a_A^{\dagger 2})}{\sqrt{2}} |\mathrm{vac}\rangle_1 = \frac{|2_D, 0_A\rangle_1 + e^{i\phi} |0_D, 2_A\rangle_1}{\sqrt{2}}, \quad (1)$$

where $a_D^\dagger = 1/\sqrt{2}(a_H^\dagger + a_V^\dagger)$ and $a_A^\dagger = 1/\sqrt{2}(a_H^\dagger - a_V^\dagger)$ represent the creation operators for photons polarized diagonally and antidiagonally with respect to the rectilinear reference frame of the PBS [Fig. 1(a)]. The vacuum state is represented by $|\mathrm{vac}\rangle$ and ϕ represents a polarization-dependent phase factor. Setting the relative phase $\phi = \pi$, the state reads:

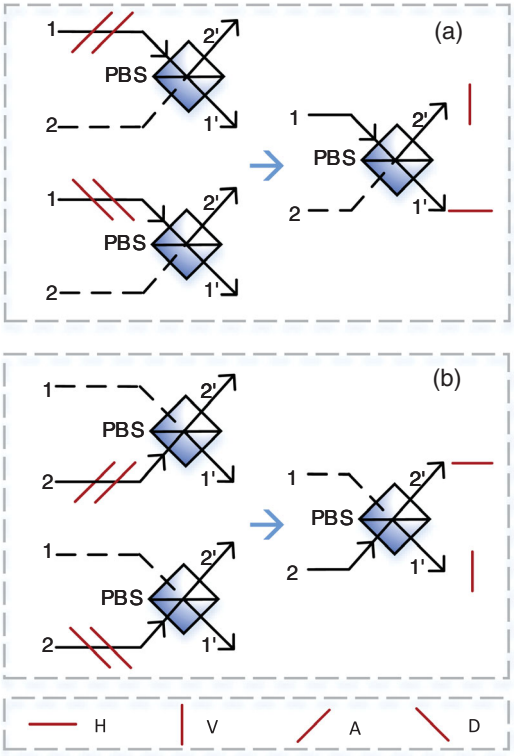

FIG. 1. Illustration of the source's principle. A pair of identical photons in a correlated state is incident on a PBS via either input port 1 (a) or 2 (b). As a consequence of time-reversed HOM interference of orthogonal polarization modes, the photons antibunch into the output ports $1'$ and $2'$. Superposition of (a) and (b) thus results in a polarization-entangled state. H, V, A, and D represent horizontal, vertical, antidiagonal, and diagonal polarizations, respectively.

$$\frac{|2_D, 0_A\rangle_1 - |0_D, 2_A\rangle_1}{\sqrt{2}} = |1_H, 1_V\rangle_1. \quad (2)$$

This can be seen as antibunching due to Hong-Ou-Mandel interference in the orthogonal polarization modes [34,35]. The PBS then maps the orthogonally polarized photon pairs into two distinct spatial modes:

$$|1_H, 1_V\rangle_1 \rightarrow |H\rangle_{1'} |V\rangle_{2'} \equiv |\Psi^{(1)}\rangle, \quad (3)$$

where $|H\rangle_i \equiv |1_H, 0_V\rangle_i$ and $|V\rangle_i \equiv |0_H, 1_V\rangle_i$ denote horizontal and vertical single-photon polarization states in ports $i = \{1', 2'\}$, respectively.

Analogously, when two photons in a state Eq. (2) are incident via port 2 of the PBS [Fig. 1(b)], one obtains single photons with the orthogonal polarization state:

$$|1_H, 1_V\rangle_2 \rightarrow |V\rangle_{1'} |H\rangle_{2'} \equiv |\Psi^{(2)}\rangle, \quad (4)$$

Consequently, the coherent superposition of pair-generation possibilities $|\Psi^{(1)}\rangle + |\Psi^{(2)}\rangle$ results in a

maximally polarization-entangled state in spatial modes $1'$ and $2'$:

$$|\Psi\rangle_{1',2'} = \frac{1}{\sqrt{2}}(|H_{1'}V_{2'}\rangle + |V_{1'}H_{2'}\rangle). \quad (5)$$

In our realization of this operational principle, we produce pairs of photons in a state Eq. (1) by balanced pumping a pair of crossed crystals with a relative inclination about their common propagation axis of 90°. By folding the configuration depicted in Fig. 1 into a loop, we realize spatial modes 1 and 2 as the clockwise and counterclockwise propagation modes of a polarization Sagnac interferometer. The polarization-entangled state Eq. (5) is then obtained by bidirectionally pumping the two crystals, which are placed in the center of the loop. This implementation thus ensures constant phases in states Eqs. (1) and (5) without any requirement for active interferometric stabilization (changes of the optical path length are experienced by the pump driving the SPDC process as well as the emitted biphoton state). Another benefit reveals itself when considering the multimode spatiotemporal characteristics of the biphoton wave packets [36]: due to the symmetric Sagnac configuration, there is, in principle, no requirement to remove distinguishing arrival-time information (e.g., via birefringent compensation crystals), as it is never created in the first place. Hence, the scheme can, in principle, also be extended to large SPDC bandwidths, and even nondegenerate wavelengths. Note that, while the scheme can also be realized using a nonpolarizing beam splitter, the implementation with a PBS automatically ensures that the correct polarizations are sorted into the two output ports, thus improving the fidelity of the polarization-entangled state. This feature can also be interpreted as an entanglement purification step [37], wherein the state impurity due to residual distinguishing information in the interfering modes merely affects the antibunching probability. Imperfect indistinguishability thus reduces the antibunching probability, and consequently the rate of joint detections in spatial modes $1'$ and $2'$. However, it should, in principle, not affect the quality of the polarization correlations conditioned on a joint detection in these two modes.

Experiment.—In our experimental realization of the source design (Fig. 2), a pair of crossed ppKTP crystals is placed inside a Sagnac loop configuration and pumped with a 405 nm continuous wave grating-stabilized laser diode. A half-wave plate (HWP) in the pump beam is used to set a diagonal polarization state, such that both clockwise and counterclockwise directions of the interferometer are pumped equally. To achieve the desired diagonal and antidiagonal polarizations within the Sagnac loop, we designed an oven with a V groove such that the two crossed crystals are oriented at [45° (see inset of Fig. 2). Thus, the crystals are phase matched for SPDC with diagonally and antidiagonally polarized pump light, respectively. The crossed-crystal configuration at the center of the loop is based on two mutually orthogonally oriented

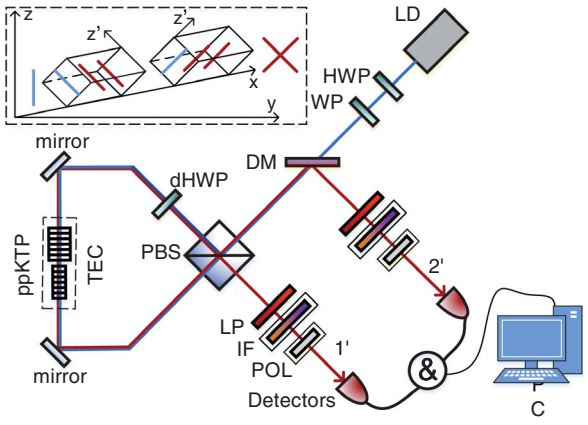

FIG. 2. Illustration of the crossed-crystal Sagnac source. LD, laser diode; PBS, polarization beam splitter; dHWP, dual-wavelength half-wave plate; HWP, half-wave plate; WP, wave plate; DM, dichroic mirror; ppKTP, type-0 periodically poled potassium titanyl phosphate crystal; TEC, temperature controller; LP, long pass filter; IF, interference filter; POL, polarizer. The top left-hand inset illustrates the 45° orientation of the oven, which ensures that photon pairs are generated either with diagonal or antidiagonal polarizations.

11.48-mm-long ppKTP crystals. They provide type-0 collinear phase matching with pump (p), signal (s), and idler (i) photons at center wavelengths of $\lambda_p \approx 405$ nm and $\lambda_{s,i} \approx 810$ nm at a temperature of 107° C. Since the pump beam in the clockwise (counterclockwise) propagation direction is horizontally (vertically) polarized, it is equally likely to generate a photon pair in the first crystal or the second crystal, resulting in a state of Eq. (1). The relative polarization phase was tuned by tilting a wave plate (WP) with optical axis set at 45°.

After combining the SPDC photon pairs from both propagation directions on the PBS, the down-converted signal and idler photons in spatial mode $2'$ are separated from the pump by using a dichroic mirror and coupled into single mode fibers. Two long-pass filters are used to eliminate the remaining pump light and noise. Polarizers are used to evaluate polarization correlations and bandpass filters are utilized to adjust the spectral bandwidth of the generated entangled state. Finally, the down-converted photons are detected by silicon avalanche photo diodes, and twofold events are identified using a fast electronic AND gate when two photons arrive at the detectors within a coincidence window of ∼3 ns.

Results.—In order to evaluate the source brightness, we removed the polarizers from the setup and set the pump laser power to approximately 100 μW. With two 3 nm bandpass filters in place, we detect a twofold coincidence rate of $R_c \approx 16$ kcps and single count rates of $R_s \approx R_i \approx 86$ kcps. This corresponds to a normalized pair rate of 160 kcps/mW, a spectral brightness of 53 kcps mW^{-1} nm^{-1}, and a heralding efficiency of $(R_c/R_s) \approx (R_c/R_i) \sim 18.5\%$ for the idler and signal photons.

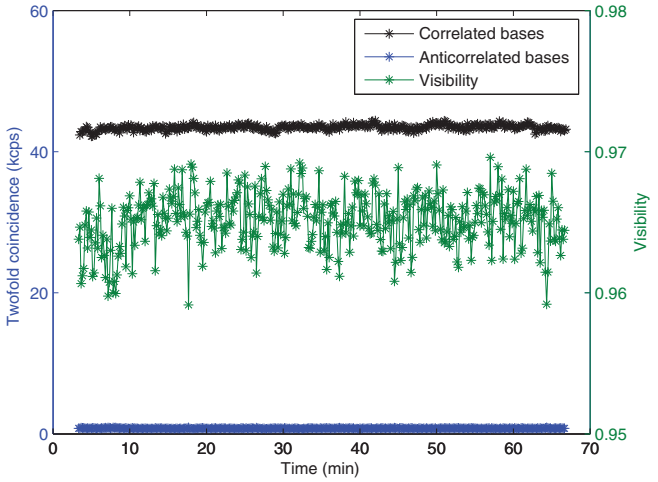

FIG. 3. Stability of our source over long time under laboratory conditions. The twofold coincidence counts and visibilities in correlated and anticorrelated A/D bases are stable on the order of hours, indicating its suitability for long-term operation in field experiments.

Next, we characterized the polarization entanglement by measuring the two-photon polarization interference contrast in two mutually unbiased bases. We observe fringe visibilities of $V_{H/V} = 99.3\%$ (99.7%) in the H/V basis and $V_{A/D} = 98.1\%$ (98.6%) in the A/D basis without (with) subtraction of accidental coincidences. These visibilities imply lower bounds of $F \geq 0.992$ and $\mathcal{C} \geq 0.984$ on the Bell-state fidelity and concurrence, respectively [38].

We also assessed the source performance without the additional 3 nm bandpass filters in place. Collecting photon pairs for the entire phase-matching bandwidth for wavelength-degenerate type-0 SPDC (~20 nm FWHM), the normalized pair rate is increased to 1.07 Mcps/mW and the spectral brightness remains essentially unchanged at 53 kcps $\mathrm{mW}^{-1}\,\mathrm{nm}^{-1}$. However, the Bell-state fidelity is reduced to $F \sim 0.88$. This reduction is mainly due to the diminished visibility in the A/D basis of 78%, which indicates that there remains a residual degree of distinguishability in the time-frequency domain.

In a perfectly symmetric Sagnac loop, the relative phase of clockwise and counterclockwise propagating pairs should be perfectly matched. We thus attribute the remaining wavelength-dependent phase to nonideal optical components, the most likely candidates being either polarization-dependent group velocity dispersion of the broadband multilayer mirror coatings or the dual-wavelength PBS, which was designed for a narrow wavelength range around 810 nm. We believe that it should be possible to obtain high visibility for the full spectrum by incorporating appropriate zero-phase-shift optical components.

To verify the long-time stability of our source, we performed measurements in the correlated and anticorrelated A/D polarization bases over the course of 1 h (Fig. 3). The results illustrate the good temporal stability of the source efficiency, as well as the quality of the entangled state, making it a suitable source for long-term autonomous operation.

Discussion.—We have demonstrated a novel entangled photon source configuration based on time-reversed HOM interference to passively route indistinguishable photons into two spatial modes. The proposed source allows the use of efficient type-0 SPDC in bulk ppKTP in a wavelength-degenerate QPM scheme, without the usual requirement for detection postselection. In particular, the recent advances in satellite-based quantum communication [28–30], and proposals for space link experiments with extreme loss [31–33], have highlighted the need for ultrabright, resource-efficient quantum sources with compact footprint and long-term stability.

Our source yields entangled photon rates in excess of 10^7 pairs per second for pump powers readily attainable using compact laser diodes, making it an ideal candidate for a variety of applications. We note that, by using a more tightly focused pump beam we could drastically improve the brightness; in principle, we expect our source to be capable of producing pair rates as high as those reported for nondegenerate phase matching [4,14], which could be of particular relevance in the development of ultrabright space-proof entangled photon sources.

While our experimental realization is based on bulk optics, the overall scheme could also be extended to integrated quantum sources, where the separation of copropagating photons with overlapping spatial modes poses a significant challenge.

We also note that the time-reversed HOM could also be extended to yield other forms of entanglement, e.g., frequency-polarization hyperentanglement or high-dimensional orbital angular momentum entanglement [39]. Another promising line of inquiry could address the combination with entanglement by path identity [40]. Finally, we also envisage the use of this approach in engineering multiphoton entanglement [41], where unbalanced beam splitting ratios could enable the filtration and tailoring of desired photon number characteristics [42,43].

In conclusion, we hope that our results will inspire new experimental configurations based on multiphoton interference. We believe that fully harnessing HOM interference could provide valuable generating and detecting complex forms of high-dimensional multiphoton entanglement, as required for the next generation of multipartite quantum information processing protocols.

We thank Thomas Scheidl and Johannes Handsteiner for helpful conversations and comments on the initial draft of the manuscript as well as Valerio Pruneri for providing ppKTP crystals. Y. C. thanks Lijun Chen for support. Financial support from the Austrian Research Promotion

Agency (FFG) Projects—Agentur für Luft- und Raumfahrt (FFG-ALR Contracts No. 6238191 and No. 866025), the European Space Agency (ESA Contract No. 4000112591/14/NL/US), as well as the Austrian Academy of Sciences is gratefully acknowledged. Y. C. acknowledges personal funding from Major Program of National Natural Science Foundation of China (No. 11690030 and No. 11690032), National Key Research and Development Program of China (2017YFA0303700), the National Natural Science Foundation of China (No. 61771236), and from a Scholarship from the China Scholarship Council (CSC).

*chenyy@smail.nju.edu.cn
†Current address: Quantum Engineering Technology Labs, H. H. Wills Physics Laboratory and Department of Electrical and Electronic Engineering, University of Bristol, Merchant Venturers Building, Woodland Road, Bristol BS8 1UB, United Kingdom.
‡Rupert.Ursin@oeaw.ac.at

[1] A. De Touzalin, C. Marcus, F. Heijman, I. Cirac, R. Murray, and T. Calarco, European Commission (2016).
[2] M. Giustina, M. A. Versteegh, S. Wengerowsky, J. Handsteiner, A. Hochrainer, K. Phelan, F. Steinlechner, J. Kofler, J.-Å. Larsson, C. Abellán *et al.*, Phys. Rev. Lett. **115**, 250401 (2015).
[3] L. K. Shalm, E. Meyer-Scott, B. G. Christensen, P. Bierhorst, M. A. Wayne, M. J. Stevens, T. Gerrits, S. Glancy, D. R. Hamel, M. S. Allman *et al.*, Phys. Rev. Lett. **115**, 250402 (2015).
[4] F. Steinlechner, S. Ramelow, M. Jofre, M. Gilaberte, T. Jennewein, J. P. Torres, M. W. Mitchell, and V. Pruneri, Opt. Express **21**, 11943 (2013).
[5] H. S. Poh, S. K. Joshi, A. Cerè, A. Cabello, and C. Kurtsiefer, Phys. Rev. Lett. **115**, 180408 (2015).
[6] P. G. Kwiat, K. Mattle, H. Weinfurter, A. Zeilinger, A. V. Sergienko, and Y. Shih, Phys. Rev. Lett. **75**, 4337 (1995).
[7] P. G. Kwiat, E. Waks, A. G. White, I. Appelbaum, and P. H. Eberhard, Phys. Rev. A **60**, R773 (1999).
[8] B.-S. Shi and A. Tomita, Phys. Rev. A **69**, 013803 (2004).
[9] M. Fiorentino, C. E. Kuklewicz, and F. N. Wong, Opt. Express **13**, 127 (2005).
[10] T. Kim, M. Fiorentino,, and F. N. C. Wong, Phys. Rev. A **73**, 012316 (2006).
[11] S. M. Lee, H. Kim, M. Cha, and H. S. Moon, Opt. Express **24**, 2941 (2016).
[12] A. Villar, A. Lohrmann,, and A. Ling, Opt. Express **26**, 12396 (2018).
[13] A. Fedrizzi, T. Herbst, A. Poppe, T. Jennewein, and A. Zeilinger, Opt. Express **15**, 15377 (2007).
[14] F. Steinlechner, P. Trojek, M. Jofre, H. Weier, D. Perez, T. Jennewein, R. Ursin, J. Rarity, M. W. Mitchell, J. P. Torres *et al.*, Opt. Express **20**, 9640 (2012).
[15] F. Steinlechner, M. Gilaberte, M. Jofre, T. Scheidl, J. P. Torres, V. Pruneri, and R. Ursin, J. Opt. Soc. Am. B **31**, 2068 (2014).
[16] M. Jabir and G. Samanta, Sci. Rep. **7**, 12613 (2017).
[17] O. Dietz, C. Müller, T. Kreißl, U. Herzog, T. Kroh, A. Ahlrichs, and O. Benson, Appl. Phys. B **122**, 33 (2016).
[18] M. Fiorentino, S. M. Spillane, R. G. Beausoleil, T. D. Roberts, P. Battle, and M. W. Munro, Opt. Express **15**, 7479 (2007).
[19] W. Sohler, H. Herrmann, R. Ricken, V. Quiring, M. George, S. Pal, X. Yang, K. H. Luo, C. Silberhorn, F. Kaiser *et al.*, *Information Optoelectronics, Nanofabrication and Testing* (Optical Society of America, Washington, DC, 2012), pp. IF1A–1.
[20] S. Krapick, H. Herrmann, V. Quiring, B. Brecht, H. Suche, and C. Silberhorn, New J. Phys. **15**, 033010 (2013).
[21] P. Vergyris, F. Kaiser, E. Gouzien, G. Sauder, T. Lunghi, and S. Tanzilli, Quantum Sci. Technol. **2**, 024007 (2017).
[22] N. Matsuda, H. Le Jeannic, H. Fukuda, T. Tsuchizawa, W. J. Munro, K. Shimizu, K. Yamada, Y. Tokura, and H. Takesue, Sci. Rep. **2**, 817 (2012).
[23] C. Clausen, F. Bussieres, A. Tiranov, H. Herrmann, C. Silberhorn, W. Sohler, M. Afzelius, and N. Gisin, New J. Phys. **16**, 093058 (2014).
[24] F. Steinlechner *Sources of Photonic Entanglement for Applications in Space* (Universitat Politècnica de Catalunya, 2015).
[25] J. Chen, K. F. Lee,, and P. Kumar, Phys. Rev. A **76**, 031804 (2007).
[26] H. Jin, F. M. Liu, P. Xu, J. L. Xia, M. L. Zhong, Y. Yuan, J. W. Zhou, Y. X. Gong, W. Wang, and S. N. Zhu, Phys. Rev. Lett. **113**, 103601 (2014).
[27] R. P. Marchildon and A. S. Helmy, Laser Photonics Rev. **10**, 245 (2016).
[28] J. Yin, Y. Cao, Y.-H. Li, S.-K. Liao, L. Zhang, J.-G. Ren, W.-Q. Cai, W.-Y. Liu, B. Li, H. Dai *et al.*, Science **356**, 1140 (2017).
[29] S.-K. Liao, W.-Q. Cai, W.-Y. Liu, L. Zhang, Y. Li, J.-G. Ren, J. Yin, Q. Shen, Y. Cao, Z.-P. Li *et al.*, Nature (London) **549**, 43 (2017).
[30] S.-K. Liao, H.-L. Yong, C. Liu, G.-L. Shentu, D.-D. Li, J. Lin, H. Dai, S.-Q. Zhao, B. Li, J.-Y. Guan *et al.*, Nat. Photonics **11**, 509 (2017).
[31] T. Scheidl, E. Wille, and R. Ursin, New J. Phys. **15**, 043008 (2013).
[32] X. Wang, L. Guo, L. Zhang, and Y. Liu, Opt. Commun. **310**, 12 (2014).
[33] Y. Neiman, EPJ Web Conf. **168**, 01007 (2018).
[34] M. R. Ray and S. J. van Enk, Phys. Rev. A **83**, 042318 (2011).
[35] A. Büse, N. Tischler, M. L. Juan, and G. Molina-Terriza, J. Opt. **17**, 065201 (2015).
[36] P. Trojek and H. Weinfurter, Appl. Phys. Lett. **92**, 211103 (2008).
[37] J.-W. Pan, S. Gasparoni, R. Ursin, G. Weihs, and A. Zeilinger, Nature (London) **423**, 417 (2003).
[38] F. Steinlechner, S. Ecker, M. Fink, B. Liu, J. Bavaresco, M. Huber, T. Scheidl, and R. Ursin, Nat. Commun. **8**, 15971 (2017).
[39] Y. Zhang, F. S. Roux, T. Konrad, M. Agnew, J. Leach, and A. Forbes, Sci. Adv. **2**, e1501165 (2016).

[40] M. Krenn, A. Hochrainer, M. Lahiri, and A. Zeilinger, Phys. Rev. Lett. **118**, 080401 (2017).

[41] T. Scheidl, F. Tiefenbacher, R. Prevedel, F. Steinlechner, R. Ursin, and A. Zeilinger, Phys. Rev. A **89**, 042324 (2014).

[42] K. Sanaka, K. J. Resch,, and A. Zeilinger, Phys. Rev. Lett. **96**, 083601 (2006).

[43] K. J. Resch, J. L. OBrien, T. J. Weinhold, K. Sanaka, B. P. Lanyon, N. K. Langford, and A. G. White, Phys. Rev. Lett. **98**, 203602 (2007).